scientific reports

Check for updates

OPEN

Numerical simulation on 90° impact test of aluminium alloy wheel with the effect of tyre

Guangdong Zhang[1]✉, Shike Tao[1], Yangyang Zhou[2], Jianjun Lu[2], Risheng Li[2], Shihui Li[2], Linzhen Zhou[1] & Tong Deng[3]

Car wheels are crucial to automobile safety, requiring a rigorous test before production. A 90° impact test simulates the frontal impact and its influences on the wheel structure, replicating dynamic driving conditions. A novel modelling approach is illustrated for the 90° impact test simulation and investigates the feasibility of excluding the tyre. Firstly, the test performs and validates five impact simulations, with the maximum deformation error being 7.04%. Subsequently, with additional tests, the effectiveness of the modelling approach is evaluated. Lastly, the effect of tyres has been analysed from an energy perspective. The results indicate that the tyre significantly influences the simulation results and should be included in the finite element (FE) model, which differs from the 13° impact test.

Keywords Car wheels; 90° impact test; Finite element model; Tyre

The wheel is a critical component that significantly influences automobile safety, typically under critical dynamic conditions while in operation. For safety, the wheel must pass restrictive tests before production. The released standards of wheel stipulate that the wheel has to pass cornering and radial tests to evaluate durability[1], with additional requirements for the light alloy wheel to pass 13° and 90° impact tests[2,3]. Crashworthiness design criteria are of even greater importance for structures designed to withstand impact conditions[4], typically validated through the impact test to assess structural safety performance.

For the impact tests, the wheel mount hub is fixed to a support structure, and a hammer impacts on either the side or the tyre tread. The hammer weight and the falling height are specified in the standards, such as GB/T 36581–2018. The deformations or cracks of the wheel are measured and must remain under specified thresholds.

As one of the wheel impact tests, the 90° impact test assesses wheel strength against perpendicular impacts during driving according to the QC/T 991–2015 standard[3], which encounters road pits or frontal stone impacts. Such impacts may instantly cause wheel failure, posing significant safety hazards. Consequently, the 90° impact test is crucial for evaluating the impact performance of wheels. In the 90° impact test, the wheel-tyre assembly is mounted vertically on a rigid structure, and a flat hammer strikes the tyre tread. The manufacturer specifies the hammer's mass, and the falling height depends on the maximum static load of the wheel. The test standard specifies two levels of falling height for the hammer, and the wheel is considered to have failed the test if any of the following conditions occur:

A maximum deformation of 2.5 mm at the inner rim flange is permitted for the low falling height. For the high falling height, cracks along a maximum of 25% of the wheel circumference at the rim are permitted.

Since the test is destructive, expensive and time-consuming[5], an FE model capable of simulating the practical test is preferable as a valuable tool for evaluating wheel strength before undertaking the impact test.

So far, several studies have been conducted in the 90° impact test[6–11]. However, due to the complexity of the tyre, the computational efficiency is never good. A FE model without tyre has been presented to improve efficiency, which is commonly applied in the 13° impact simulation. In the 13° impact test, the impact occurs at the tyre sidewall and the outer rim flange, with the impact force distributed between the two. Conversely, in the 90° impact test, the hammer impacts only the tyre tread, with all the force transmitted to the rim through the tyre. The tyre undergoes large deformation during the 90° impact test, demonstrating significant nonlinearity, which leads to low simulation efficiency, particularly when the sidewall completely folds under the high-impact energy[10].

[1]School of Mechanical Engineering, Yancheng Institute of Technology, Yancheng, Jiangsu 224051, China. [2]Hebei High Strength and Toughness Lightweight Wheel Technology Innovation Center, Baoding Lizhong Wheel Manufacturing Co., Ltd., Baoding, Hebei 071000, China. [3]The Wolfson Centre for Bulk Solids Handling Technology, Faculty of Engineering and Science, University of Greenwich, ME4 4TB Chatham, UK. ✉email: gdzhang@ycit.edu.cn

Moreover, as the complexity of the tyre's structure and materials increases, simulation efficiency decreases. Compared to the 90° impact test, the tyre deformation is minor in the 13° impact test, and related studies indicate that the tyre absorbs approximately 20% of the impact energy in the 13° impact test[12]. Consequently, to enhance simulation efficiency, some researchers have reduced the impact energy of the hammer (i.e., the initial velocity of the hammer) and established a FE model of the 13° impact test without a tyre, achieving a 60% increase in simulation efficiency with minimal loss in computational accuracy[12]. However, such studies have not been found in the field of 90° impact simulations.

Using a modified FE model, a novel approach is presented for simulating the 90° impact test on aluminium wheels. This study aims to develop a simulation method that ensures efficiency and accuracy while also investigating the feasibility of excluding the tyre. Observations from impact tests indicate that tyres primarily serve a cushioning role, causing the hammer to hit the wheel-tyre assembly many times until its kinetic energy is exhausted. Given that the rim deforms most significantly after the first impact (which possesses the most impact energy), this paper establishes a FE model that accounts for a single impact process, yielding a maximum relative error of 7.04% (without considering tyre deflation), which is lower than the 8% error reported in the existing literature[10]. By establishing the 90° impact test model that considers a single impact, this paper circumvents the low simulation efficiency associated with many impacts while ensuring accuracy. The paper provides a reference method to ensure the efficiency and accuracy of the 90° impact simulation. Furthermore, the effect of the tyre on the wheel impact test and the feasibility of removing the tyre in simulation are investigated, contributing to bridging the gap in simulation methods.

Introduction of 90° wheel impact test

As shown in Fig. 1, according to the QC/T 991–2015, the 90° impact test machine consists of a supporting structure and a hammer assembly composed of a main and an auxiliary hammer. The main and the auxiliary hammer are connected by calibrated springs pre-compressed by 6 mm, with a combined spring stiffness ranges from 0.98 kN/mm to 1.3 kN/mm. In the test, the wheel mount hub is vertically fixed to a rigid supporting structure, which is rigidly connected to the ground. The hammer falls from a specific height to impact the wheel-tyre assembly to simulate the frontal impact. For instance, a wheel encounters road pits or frontal stone impacts.

Before the test, the axial and circumferential positions of the wheel are adjusted to ensure the hammer impacts the area between the rim centreline and the inner rim flange (Fig. 1). Firstly, the height of the hammer is lowered to bring it closer to the tyre and adjust the axial position of the wheel. Subsequently, the support structure is moved along the wheel's axial direction to align the centerline of the tyre's cross-section with the edge of the hammer's impact surface. Finally, the wheel is rotated so the impact area (typically where the valve hole is located) is positioned under the hammer.

After adjusting the testing machine, the hammer is lifted to a specified height and released to hit the wheel. During the test, the tyre undergoes large deformation, with part of the impact energy absorbed by the tyre to replicate its cushioning effect, while the rest is absorbed by the wheel, resulting in significant rim deformation. At the end of the impact process, the hammer is lifted and separated from the tyre to ensure the rim restores elastic deformation. After about one minute, the plastic deformation of the inner rim flange is measured, which is used to assess the stiffness of the rim and guide designers on whether the optimisation design is necessary. The method for measuring the deformation of the inner rim flange is shown in Fig. 2. Moreover, according to the measurement method specified by QC/T 991–2015, rim deformation is defined as the difference between the rim diameters at the impact point before and after the impact.

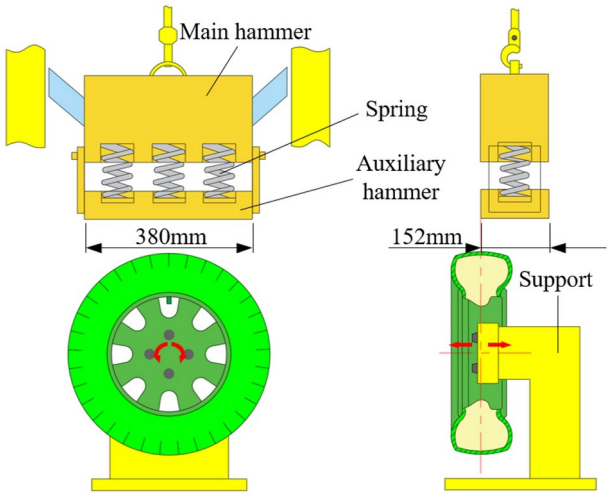

Fig. 1. The setup of the 90° impact test.

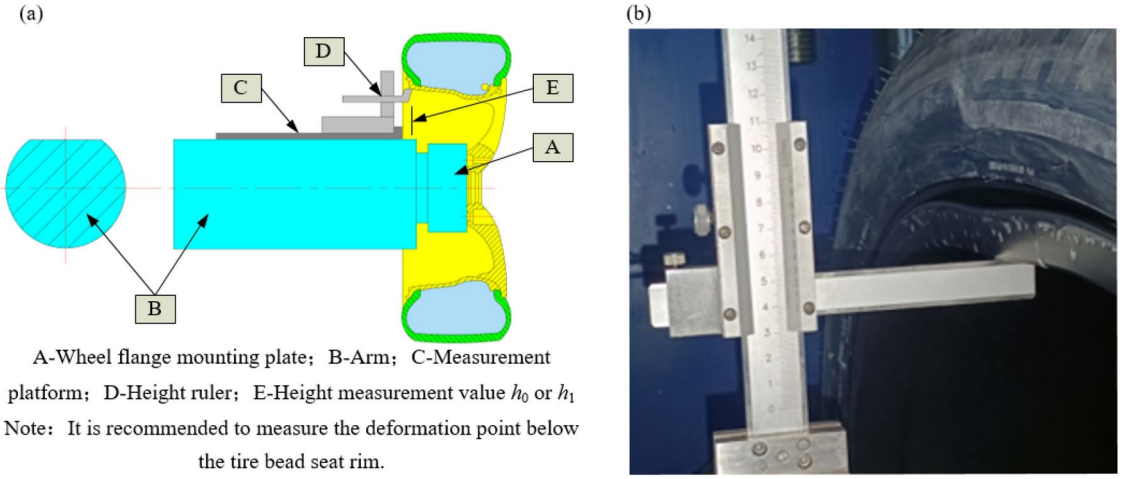

Fig. 2. The measurement of deformation. (**a**) Measurement method, (**b**) Measurement of inner rim flange deformation.

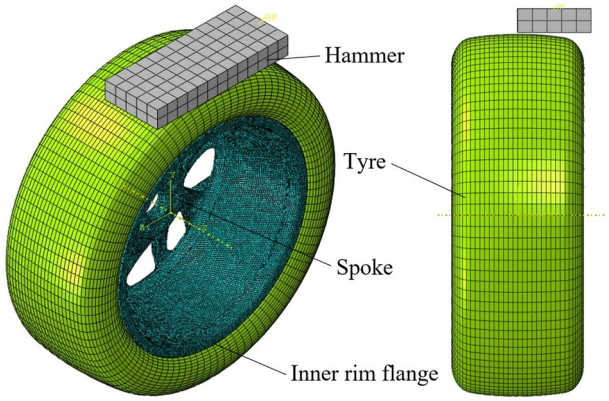

Fig. 3. FE model of 90° model.

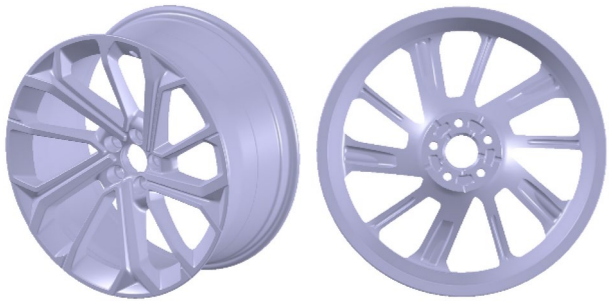

Fig. 4. The geometric model of the wheel.

Development of FE model

A novel FE model to simulate the 90° impact test has been developed using the means of commercial software "HyperMesh" and "Abaqus". The model comprises a wheel, tyre, and hammer, as shown in Fig. 3. The wheel (as shown in Fig. 4) and the matching tyre are 20 × 9.0 J and 275/45 R20, respectively.

The initial moment of the wheel impact simulation occurs when the hammer contacts the tyre. Since the tyre needs to be inflated prior to the impact simulation, and tyre inflation causes tread displacement, a specific distance between the tread and the hammer has been left in advance to ensure that the tyre is fully inflated without any interference. The distance is determined through inflation simulations, yielding a value of 3.5 mm.

Additional information, including material properties, load, boundary conditions, and types of contact, can be found in Sections "Materials" to "Load and boundary conditions".

Materials

Tyre

In the 90° impact test, the hammer directly hits the tyre, and the impact force ultimately transmits through the tyre to the wheel, highlighting the tyre's crucial role. The challenges of modelling the tyre are mainly the complexity of the structure, material composition, and material nonlinearity[13–15], considered the most complex aspects of the impact process[16]. However, the purpose of the 90° impact test is to test the wheel, not the tyre. A detailed model of the tyre will be out of the FE model for the 90° impact test. So, a simplified tyre model comprising rubber, bead, carcass and belt is developed, as shown in Fig. 5. The carcass and the belt, so-called layers, are embedded in the tyre, surrounded by rubber material.

Due to the large deformation of tyres during the impact process, the selection of rubber material is crucial. Common rubber materials used in wheel impact tests include the Mooney-Rivlin model[7,8,10]and the Yeoh model[9,17]. The material test for the Mooney-Rivlin model only includes uniaxial test, whereas the Yeoh model's test includes uniaxial test, biaxial test, and shear test, according to the ANSYS Engineering Data (ANSYS 2022R1). In comparison, the Yeoh model features more test conditions, enabling a more comprehensive representation of various deformations of the rubber material. Relevant studies suggest that, under the conditions of large deformation in rubber, the Yeoh model more accurately approximates the material's constitutive relationship compared to the Mooney-Rivlin model[18]. Given that the tyre undergoes significant and complex deformations during the impact test, the Yeoh model is more appropriate for this study, specifying a 1200 kg/m^3 density.

Due to the experimental limitations, the data for the Yeoh model are taken from the ANSYS Material Library (ANSYS 2022R1). ANSYS possesses a comprehensive materials database, including rubber materials, which significantly enhances experimental data acquisition. The Yeoh model comprises three coefficients (C_{10}, C_{20}, C_{30}) and can be acquired through the material evaluation function of Abaqus, which is just one data fitting method. If conditions permit, the coefficients can also be fitted using alternative methods, such as mathematical software for data fitting.

Through the material evaluation function of Abaqus, the Yeoh coefficients (unit: MPa) are acquired, which are $C_{10}=0.771$, $C_{20}=-0.386$, and $C_{30}=0.197$. The simulation does not account for the strain rate dependency of rubber material[19,20].

Following the discussion of the rubber material, descriptions of other materials are provided below. In the tyre model, the bead is modelled by an isotropic material with a cross-section of 5 mm × 5 mm. The material density is 7800 kg/m^3; the Young's modulus is 210 GPa; the Poisson's ratio is 0.3. The carcass and the belt are embedded in tyres, which are modelled with layers of equally spaced fibre reinforcements. The material parameters of the carcass and the belt are taken from the literature[9].

This tyre model has been verified with the material parameters adjusted based on testing and simulation, considering the tyre's crucial role in transmitting the impact force to the wheel. A study of a 90° impact test under 228 mm falling height condition has been conducted (as shown in Fig. 6) to minimise the error of inner rim flange deformation between simulation and test, thereby adjusting the material parameters of the tyre model. The result is shown in Fig. 7, and the material parameters are given in Table 1. In this test, the deformation of the inner rim flange is 19.34 mm, while the simulation value is 20.38 mm, indicating an error of 5.38%. The result indicates that the adjusted tyre material parameters cause a small error in the inner rim flange deformation between simulation and test and ensure the accuracy of the tyre model.

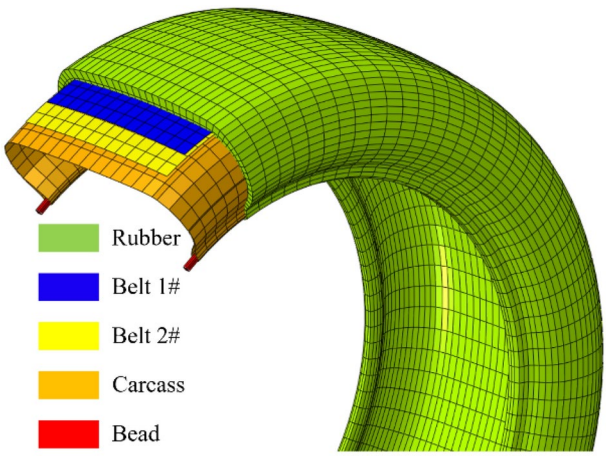

Figure 5: Tyre model

Fig. 5. Tyre model.

Fig. 6. 90° wheel impact test.

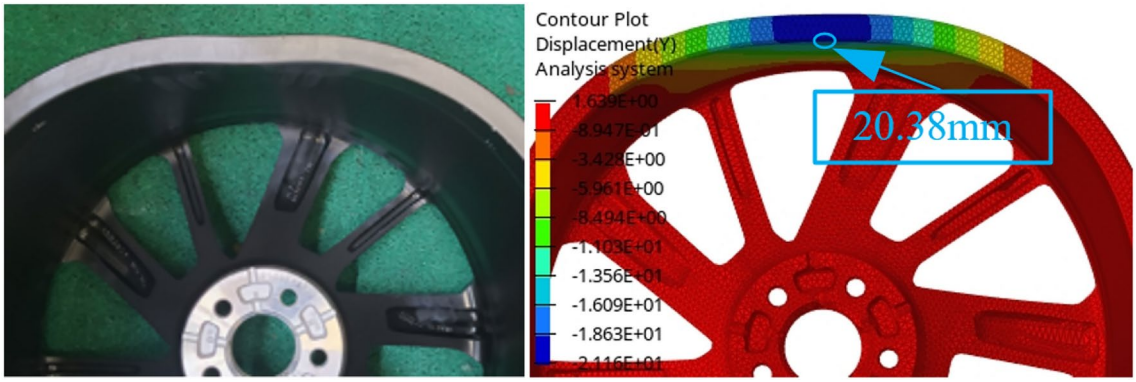

Fig. 7. Test and simulation result.

Material name	Young's modulus (GPa)	Poisson's ratio	Material density (kg/m^3)	Section area (mm^2)	Cord spacing (mm)	Angle with the tyre meridian plane (degree)
Carcass	10	0.4	1200	0.241	1	0
Belt 1#	200	0.3	7800	0.141	1.176	63
Belt 2#	200	0.3	7800	0.141	1.176	117

Table 1. Cord material parameters.

Car wheel

The wheel material used for modelling is aluminium alloy, of which the density is 2700 kg/m^3; the Young's modulus is 71 GPa; the Poisson's ratio is 0.33.

Because the maximum impact stress on the wheel in the test exceeds the yield limit of aluminium alloy, the hardening characteristic must be included, which exhibits the material's characterisation after the stress exceeds its yield limit. Since the impact area in the 90° impact test is near the inner rim flange and far from the spoke, which is different from the 13° impact tests where the impact area is the outer rim and the spoke, the material property of the spoke is ignored. The specimen is extracted from the inner rim flange, and the hardening curve is obtained from the tensile stress test, as shown in Fig. 8.

Hammer

In the impact test, the spring between the main and the auxiliary hammer is cushioned to absorb the impact energy. The first impact force can be high, and the duration can be short, so the spring may not provide a cushion promptly. Using the Abaqus/Explicit software to simulate the instantaneous impact, with the complexity

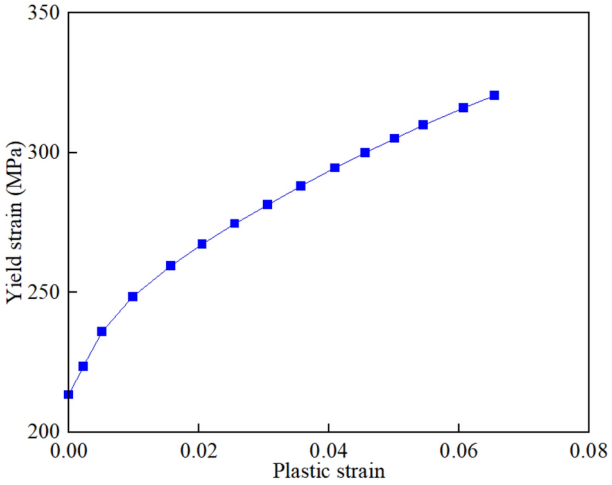

Fig. 8. Hardening characteristic of the aluminium alloy.

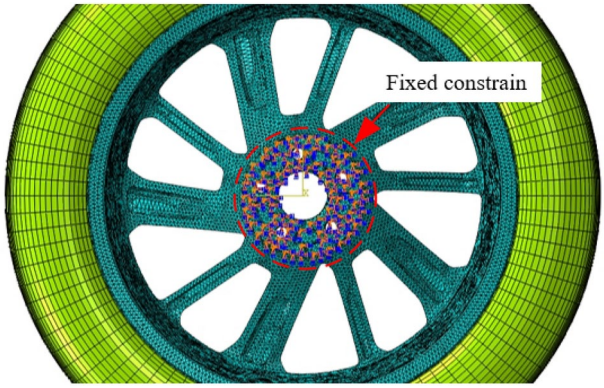

Fig. 9. The fixed constraint on the hub.

of repeated impacts and the cushioning effect of springs, the simulation may take prolonged computational time. Therefore, the first impact is simulated without considering the spring's effect to enhance computational efficiency, enabling the main and auxiliary hammers to be modelled as a whole.

The mass of the hammer is 1010 kg. According to the QC/T 991–2015 standard, a hammer model whose dimensions are 380 mm × 152 mm × 50 mm is established, with a virtual density of 3.5×10^5 kg/m^3.

Supporting structure

Since the wheel mount hub is fixed to a rigid support, and the support is connected to the ground rigidly, a fixed constraint is applied on the hub, and the bolt preloading is ignored, as shown in Fig. 9, thereby ignoring the supporting structure to reduce the complexity of FE model.

Meshing process

The FE model for wheel and tyre pre-processing is completed in "HyperMesh" software to prevent the explicit solver from abortion due to excessively distorted elements.

The wheel is discretised with 4-node tetrahedral elements of 5 mm in size. The criteria for evaluating element quality include skewness, aspect ratio, Jacobian ratio, etc. Poor quality elements can be manually improved based on these criteria to enhance their quality. The aspect ratio of the element is shown in Fig. 10. The threshold for the aspect ratio is set to 100, indicating that there are nine elements with aspect ratios greater than 100. These elements have been marked by "HyperMesh" and then corrected manually, as shown in Fig. 11.

Subsequently, the half cross-section of the tyre (including beads) is discretised manually, followed by rotation and mirroring operations to create 3-dimensional tyre elements, as shown in Fig. 12.

Because the hammer's stiffness is significantly greater than the tyre and the wheel, and the hammer's mechanical response is not the study's focus, the hammer is constrained as a rigid body with an element size of 30 mm. The element size for the belt and carcass is set to 15 mm. The result is shown in Fig. 13.

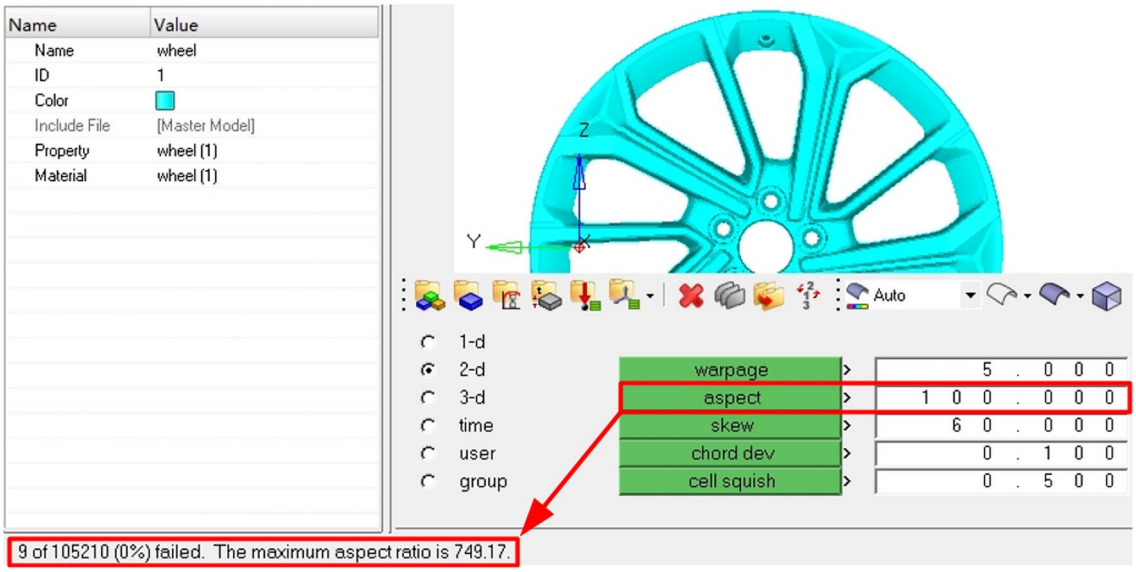

Fig. 10. The results of the aspect ratio of elements.

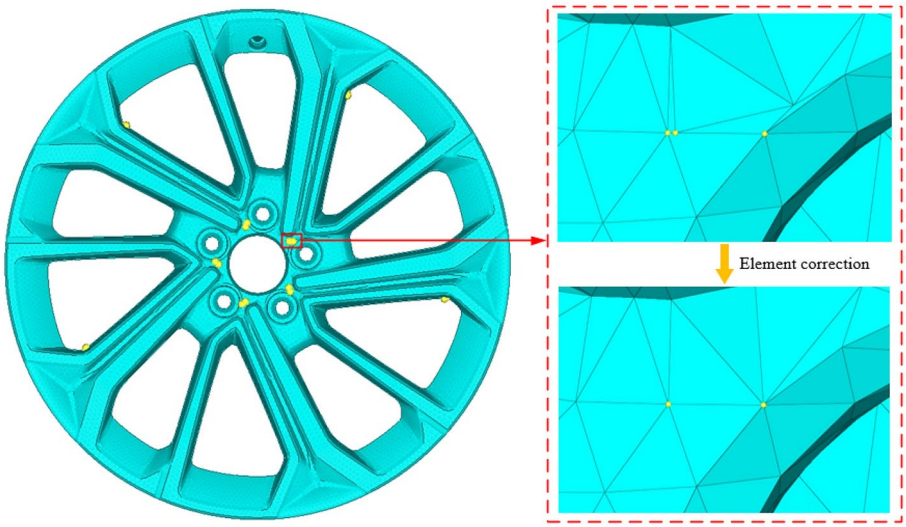

Fig. 11. The process of element quality improvement.

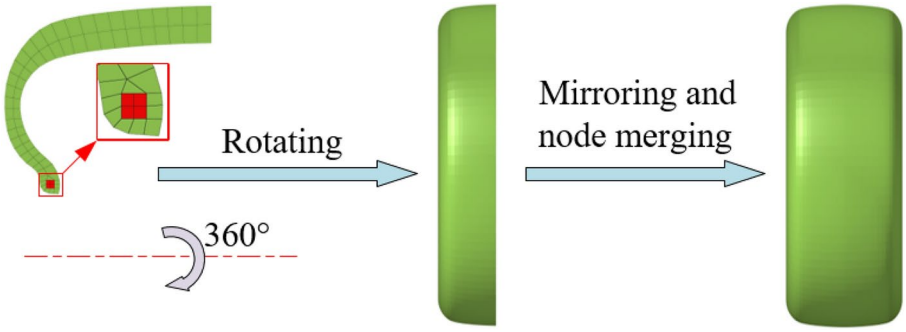

Fig. 12. Three-dimensional tyre elements.

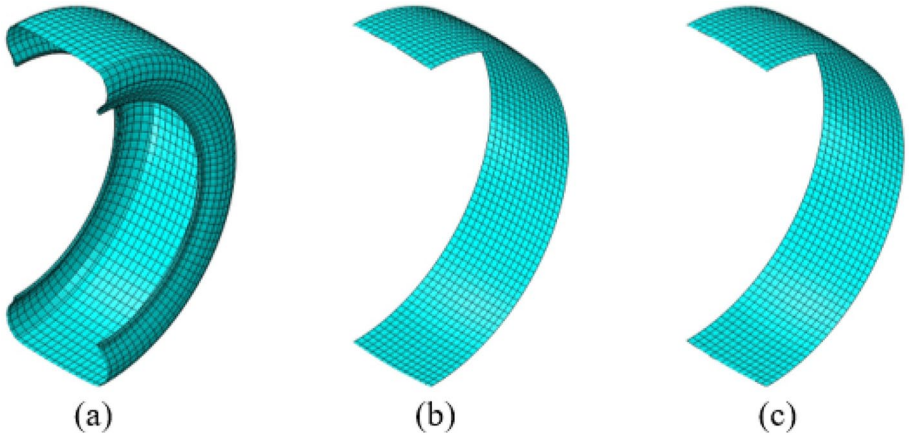

Fig. 13. Meshing results. (**a**) Carcass, (**b**) Belt 1#, (**c**) Belt 2#.

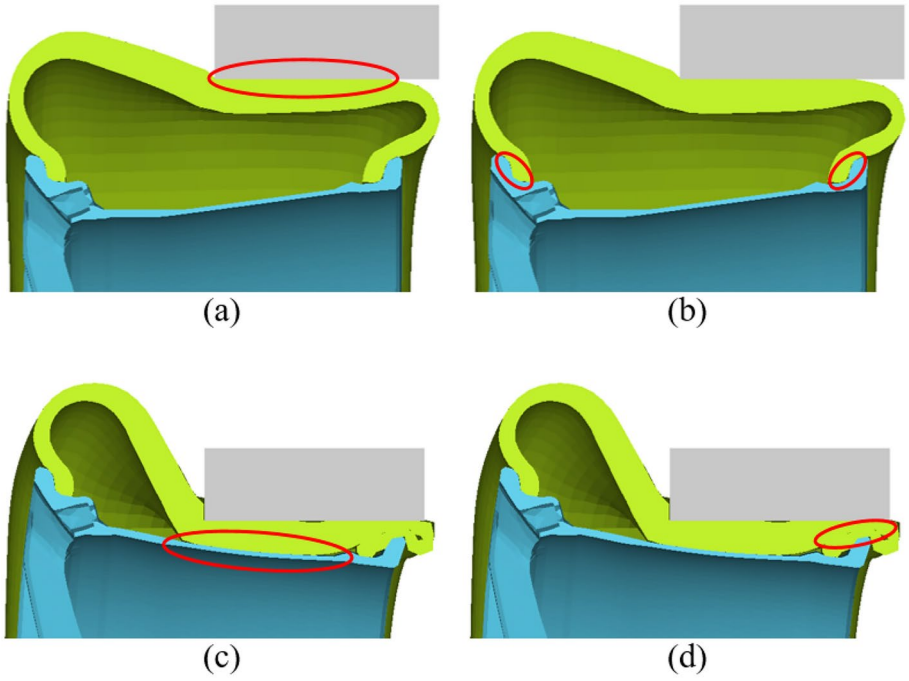

Fig. 14. The type of contact during the impact process. (**a**) The contact between tread and hammer, (**b**) The contact between bead and flange, (**c**) The contact between tyre and rim, (**d**) The self-contact of tyre.

Load and boundary conditions

In the FE model, the stiffening effect by tyre inflation pressure is introduced by applying a uniform pressure of 0.255 MPa on the inner surface of the cavity surrounded by the tyre and the rim. The influence of Earth's gravity is considered. A fixed constraint is applied to the wheel mount hub (Fig. 9). The hammer is imposed by an initial velocity obtained from the theory as indicated in Eq. (1).

$$\nu = \sqrt{2gh} \tag{1}$$

where h is the falling height of the hammer, and g is the gravity acceleration (9.8 m/s^2).

Five sets of tests and simulations have been conducted, with different falling heights of the hammer of 199 mm, 209 mm, 228 mm, 237 mm, and 246 mm. Therefore, the initial velocities of the hammer are 1974.9 mm/s, 2024.0 mm/s, 2114.0 mm/s, 2155.3 mm/s, and 2195.8 mm/s respectively.

Because of the short duration of the impact, the little energy loss caused by friction[21], and the complexity of the contact during the impact process, as shown in Fig. 14, a general contact option which takes into account

self-contact due to the large deformation of the tyre, with contact attributes set to 'Normal Hard Contact and Tangential Frictionless' is used to detect the contacting surface responses during simulation.

Simulation Strategy

The simulation of the 90° impact test is conducted in three steps:

(1) Inflating the tyre; (2) Assigning the initial velocity to the hammer; (3) Simulating the impact.

All steps are executed using the Abaqus/Explicit solver.

The tyre inflation was completed in 0.003 s for the first step. So, the duration of the first step is 0.003 s.

In the second step, a time interval of 1×10^{-8} s is assigned to impose the hammer with an initial velocity to neglect the falling displacement over an extremely short time.

In the third step, the impact duration is set to 0.25 s to ensure the hammer rebounds after reaching the lowest point, and the inner rim flange restores elastic deformation, allowing for the acquisition of the final plastic deformation at the impact area.

Simulation and experimental validation

During the impact process, the hammer is primarily accelerated by gravity and stopped by the reaction force generated by the wheel-tyre assembly. As a result, the velocity of the hammer initially increases and then decreases to zero. When the velocity reaches zero, the hammer stops at the lowest point and rebounds upwards due to the reaction force. During the impact, significant deformation of the inner rim flange is generated. Figure 15 shows the change of inner rim flange deformation at varied falling heights and a consistent trend of the deformations. When the impact finishes, the inner rim flange undergoes an elastic recovery due to the material characteristics, and eventually, a steady plastic deformation is achieved.

Tests were carried out to validate the simulation results (Fig. 6 of Section "Tyre"). Moreover, the rim deformations were obtained using the measurement method specified in QC/T 991–2015 (Fig. 2).

The comparison between the tests and the simulations is shown in Fig. 16 and Table 2. It shows a good agreement between the simulations and the tests, with a maximum relative difference of about 7.03%, except for the result in the 246 mm falling height condition. In the tests, air leakage was detected for the 246 mm falling height, which may result in lower air pressure in the tyre compared to other conditions. Low air pressure causes a reduction of the tyre stiffness, which leads to a sharp deformation of the inner rim flange because the hammer impacts the lowest point earlier.

The tyre pressure was adjusted to 0.2 MPa before simulation to investigate the effect of tyre stiffness on the deformation of the inner rim flange, with the result shown in Fig. 17. Figure 17 indicates that at a tyre pressure of 0.2 MPa, the deformation of the inner rim flange is 22.12 mm, which exceeds the deformation observed before the pressure reduction. The reduction in tyre pressure reduces tyre stiffness, diminishing the tyre's cushioning effect, causing the rim to endure a more significant load and increasing deformation. In tests, a reduction in tyre pressure is typically attributed to tyre deflation, which often occurs at greater falling heights, such as the 246 mm height discussed in this paper. Tyre deflation is a common failure mechanism under severe impact conditions, which has been investigated by many researchers[22]. The Tyre failure mechanism is out of this study and has not been discussed in this paper. These can be investigated in future.

More 90° impact tests have been conducted to evaluate the effectiveness of the modelling procedure developed. The wheel size is 20 × 10.0 J, instead of the 20 × 9.0 J used before, and the matching tyre is 275/35 R20 instead of 275/45 R20. The falling heights of the hammer are 43 mm and 237 mm, respectively, and the tyre inflation pressure is 0.2 MPa.

The comparison between the tests and the simulations is shown in Fig. 18, which shows an excellent agreement with relative differences of 4.84% and 5.28%, respectively. The results indicate that the FE model developed for

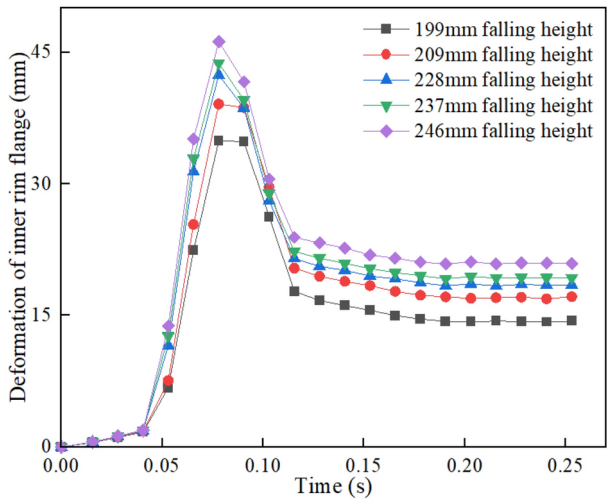

Fig. 15. The deformation of the inner rim flange in the impact test for varied falling heights.

Fig. 16. The results of the test and simulation for different levels of falling height.

Impact height (mm)	Deformation of the inner rim flange		Relative difference (%)
	Test value (mm)	Simulation value (mm)	
199	13.66	14.37	5.20
209	16.32	17.12	4.90
228	19.44	18.46	5.04
237	20.74	19.28	7.04
246	23.58	20.92	11.28

Table 2. The result of impact test and simulation.

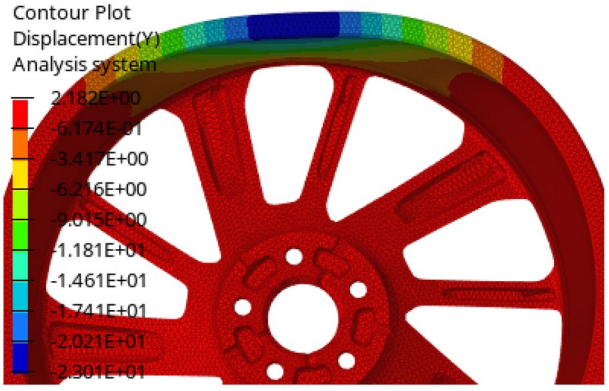

Fig. 17. The simulation result at a tyre pressure of 0.2 MPa.

the 90° impact test can predict the inner rim flange deformation with reasonable accuracy, ultimately verifying the effectiveness of the modelling procedure.

Although the simulation results may not completely correspond with the test results, improving the model's accuracy can minimise the difference between simulation and test, thereby enabling more accurate predictions of actual test outcomes and guiding designers on whether optimisation is necessary. Furthermore, this is essential for decreasing the number of prototypes and tests, ultimately reducing costs.

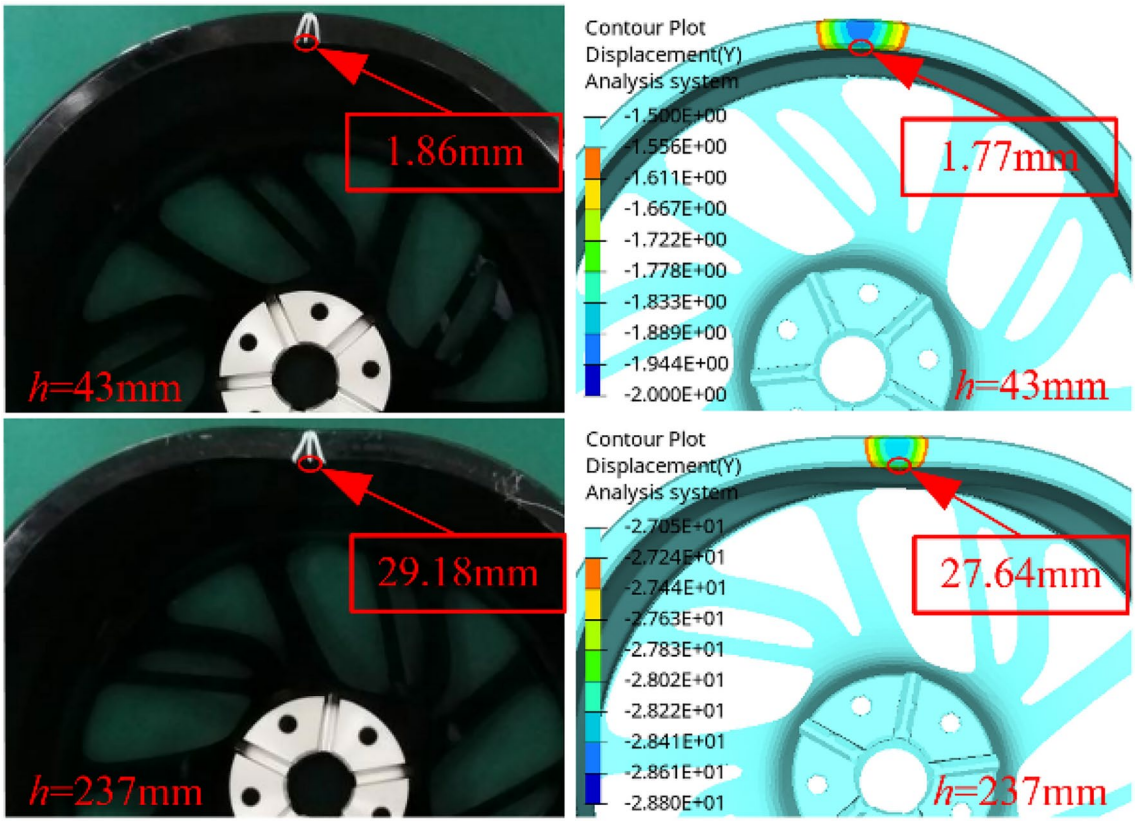

Fig. 18. The result of test and simulation.

Analysis of the tyre effect

In the simulation of the impact tests, because of the complexity of the tyre, some FE models of the 13° impact test excluded the influence of the tyres by reducing impact energy to compensate for the absence of the tyre[12] to enhance computational efficiency. The tyre plays an essential role in the 90° impact test simulation, as analysed in Section "Tyre". Using a novel simulation method, the current method takes the idea from an energy perspective forward for the effect of the tyre in the 90° impact test.

In this section, the energy absorbed by the tyre is calculated. Given the complexity of the tyre, the Law of Energy Conservation is used to calculate the energy absorbed by the tyre indirectly as follows:

If a hammer falls from a certain height and impacts a wheel-tyre assembly, when the hammer reaches the lowest point, the hammer and the wheel have an instantaneous stop. In such conditions, the kinetic energy of the hammer and the wheel is zero. Therefore, the energy absorbed by the wheel is entirely converted into internal energy of the deformation. Moreover, because the hammer is constrained as a rigid body, the internal energy of it is zero. If frictional losses in the impact are not considered, the energy absorbed by the tyre can be calculated using the Law of Energy Conservation:

$$E = mg(h_0 + h_1) \tag{2}$$

$$\Delta E_{tire} = E - \Delta E_I \tag{3}$$

where E is the total impact energy,m is the mass of the hammer, g is the gravity acceleration, h_0 is the falling height of the hammer, and h_1 is the displacement of the impact between the tread and the lowest point (as shown in Fig. 19), ΔE_{tire} is the energy absorbed by the tyre, and ΔE_I is the increased internal energy of the wheel.

When the falling height is 228 mm, the simulation results show that the impact displacement is 139.75 mm, and the increased internal energy of the wheel is 1624.80 J when the hammer reaches the lowest point. The total impact energy is 3691.95 J, calculated based on Eqs. (2) and (3), and the energy absorbed by the tyre is 2015.18 J. The absorption rate by the tyre is 55.36%. With the method developed, the energy absorbed by the tyre under other conditions can be calculated, as shown in Table 3.

Table 3 illustrates a decrease in the percentage of the energy absorbed by the tyre with an increasing falling height of the hammer, leading to the rim deforming sharply under a more significant impact force. In particular, the impact of tyre deflation has been supplemented. The result indicates that as the tyre pressure decreases, energy absorption efficiency also decreases. For example, at an impact height of 228 mm and a tyre pressure of 0.2 MPa (as discussed in Section "Simulation and experimental validation"), the energy absorption efficiency is only 48.65%, lower than the 55.36% observed under the same height conditions.

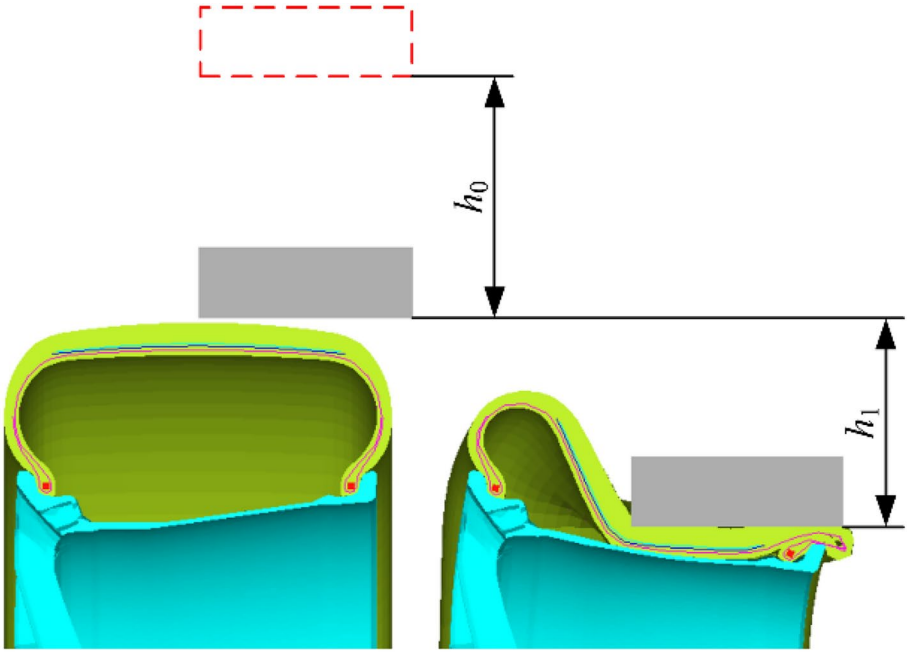

Fig. 19. Falling height and impact displacement.

Falling height(mm)	199	209	228	237	246
Impact displacement(mm)	134.92	136.44	139.75	140.47	141.65
Total energy(J)	3305.14	3484.10	3691.95	3790.93	3889.91
The increased internal energy of wheel(J)	1285.27	1388.92	1624.80	1672.77	1764.46
The energy absorbed by tyre(J)	2019.87	2030.24	2015.18	2063.42	2072.52
The ratio of energy absorbed by tyre (%)	61.11	59.38	55.36	55.23	54.01

Table 3. Energy calculation results.

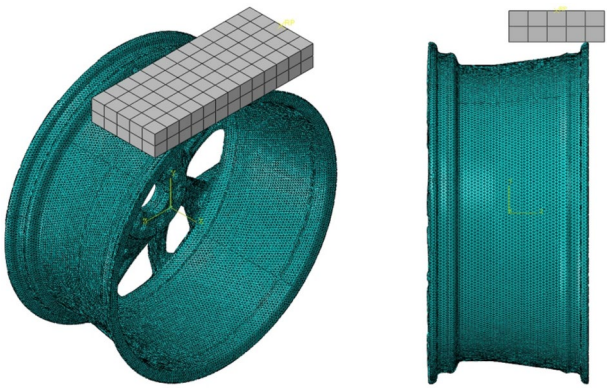

Fig. 20. The model excluding tyres.

As a comparison, a FE model is executed without a tyre, as shown in Fig. 20, in which the hammer is set to approach the inner rim flange. In Fig. 20, the model's parameters (including materials, boundary conditions, etc., as described in Sections "Materials" to "Load and boundary conditions") remain unchanged, except for tyre removal and the hammer's initial velocity change.

The feasibility of removing the tyre in 90° impact simulations will be investigated. The tyre absorbs part of the impact energy in both the 13° impact test and the 90° impact test. Therefore, when establishing an FE model that excludes the tyre, it is essential to reduce the hammer's initial velocity to compensate for the absence of the

Falling height (mm)	Deformation of the inner rim flange	
	With tyre (mm)	Without tyre (mm)
199	14.37	13.22
209	17.12	15.38
228	18.46	17.55
237	19.28	18.20
246	20.92	19.33

Table 4. The comparison of the deformations between the two models.

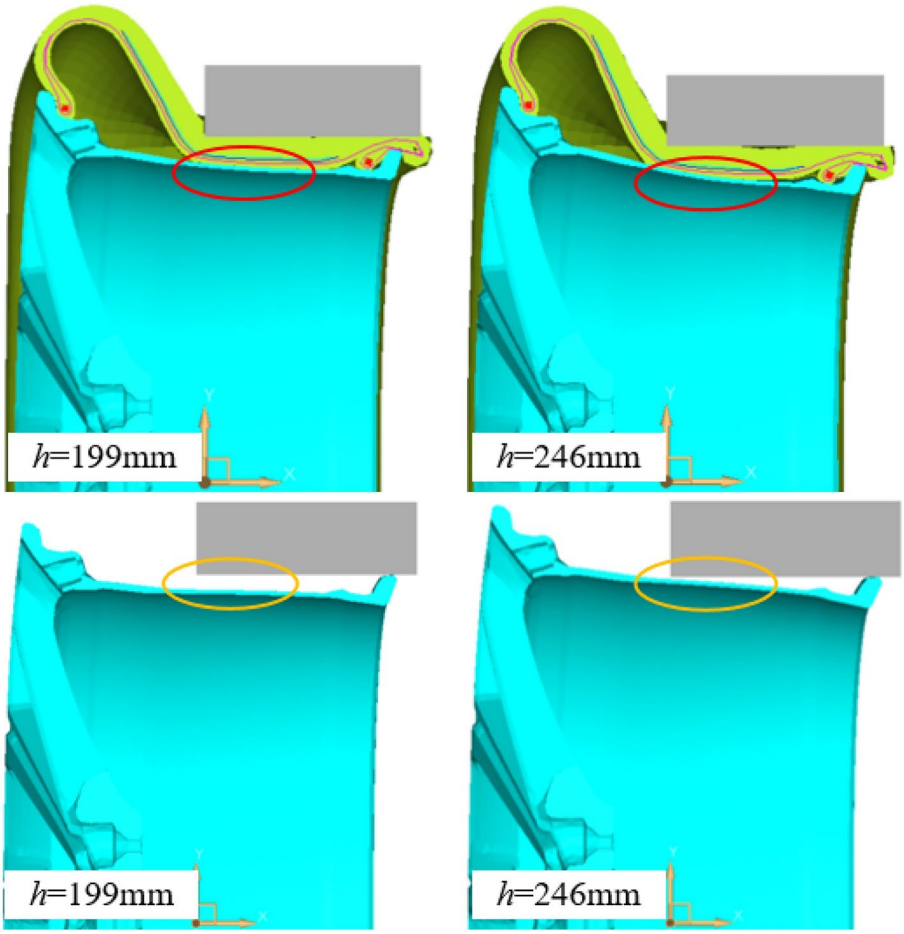

Fig. 21. The maximum deformation for the falling height at (**a**) $h = 199$ mm and (**b**) $h = 246$ mm.

tyre in the simulation. In the 90° impact simulation, the reduced initial velocity can be determined using the following equation[17]:

$$v = \sqrt{2g(1-\delta)h} \tag{4}$$

where g is the gravity acceleration, h is the falling height of the hammer, and δ is the percentage of the impact energy absorbed by the tyre (using the data shown in Table 3).

The final plastic deformations of the inner rim flange are reported in Table 4, which shows that the inner rim flange deformation values from the simulation without a tyre are uniformly more minor than the corresponding results for the simulation with a tyre. The cause of the more minor deformation is shown in Fig. 21 as the representative moment when the hammer reaches the lowest point. Figure 21 indicates that the area from the rim centreline to the inner rim flange is impacted when considering the tyre, which differs from the simulation without a tyre. This suggests that the rim is also subjected to impact when considering the tyre, and compared to the inner rim flange, the thinner thickness of the rim results in lower stiffness and more significant deformation under impact force, thereby leading to more significant deformation of the inner rim flange. Figure 22 shows the

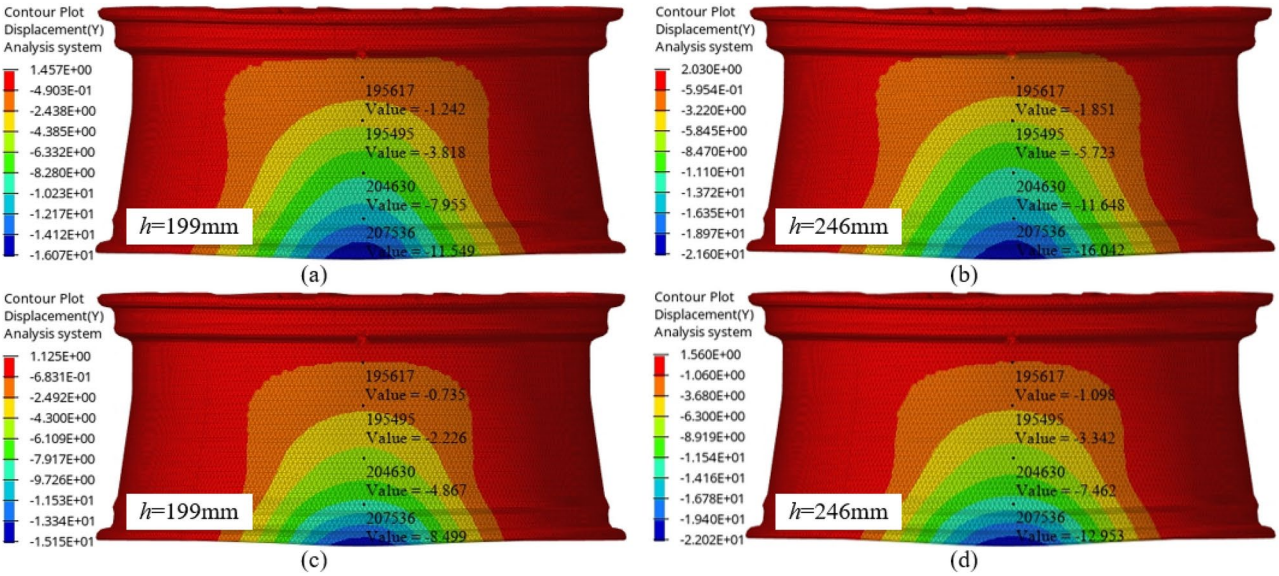

Fig. 22. Rim deformation. (**a**)~(**b**)Including tyre, (**c**)~(**d**) Excluding tyre.

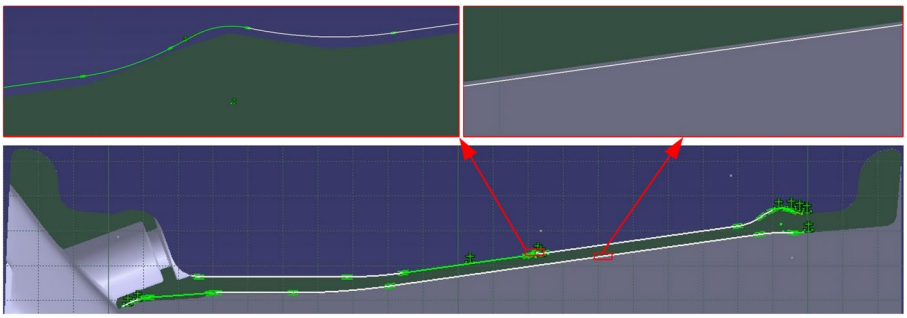

Fig. 23. The optimisation of rim structure.

details of rim deformation, from which the minor deformation can be found in the model without a tyre under the same falling height condition.

The effect of the tyre in the 90° impact test reveals that the FE model without a tyre only simulates the hammer impacting the inner rim flange and shows a minor rim deformation under the same falling height condition compared with the model with a tyre.

Also, the results in Table 3 indicate that the efficiency of the energy absorption by the tyre is related to the falling height of the hammer, further emphasising the necessary inclusion of the tyre in the 90° impact simulation. Therefore, it is necessary to include the tyre in the FE model for the 90° impact test rather than excluding it, which differs from the 13° impact simulation where the tyre can be excluded by reducing the impact energy.

Discussion

The study in this paper can guide driving safety. The analysis of energy absorbed by tyres indicates a decreased efficiency of tyre energy absorption as the hammer's falling height (or velocity) increases. Therefore, cars should pass over the road obstacles at a low speed to protect the wheel and reduce safety hazards.

Through analysis, it can be concluded that when the tyre model is omitted, the inner wheel rim flange deformation is relatively slight. When tyre models are included, the deformation of the inner rim flange increases. Optimising rim structure, such as increasing the rim thickness, as shown in Fig. 23, which is less costly and more straightforward compared to approaches like process optimisation or increasing material strength[23], may contribute to enhancing the rim stiffness, thereby reducing the deformation of rim and inner rim flange (as shown in Fig. 24).

In the real world, the instantaneous stress between the contact surfaces of the hammer and the inner rim flange may be excessively high due to the lack of tyre cushioning. Further experimental validation was not conducted for the bare wheel to prevent the test machine from being damaged and avoid potential risks. In the future, more approaches will be explored to investigate the effect of tyres in the 90° impact test further.

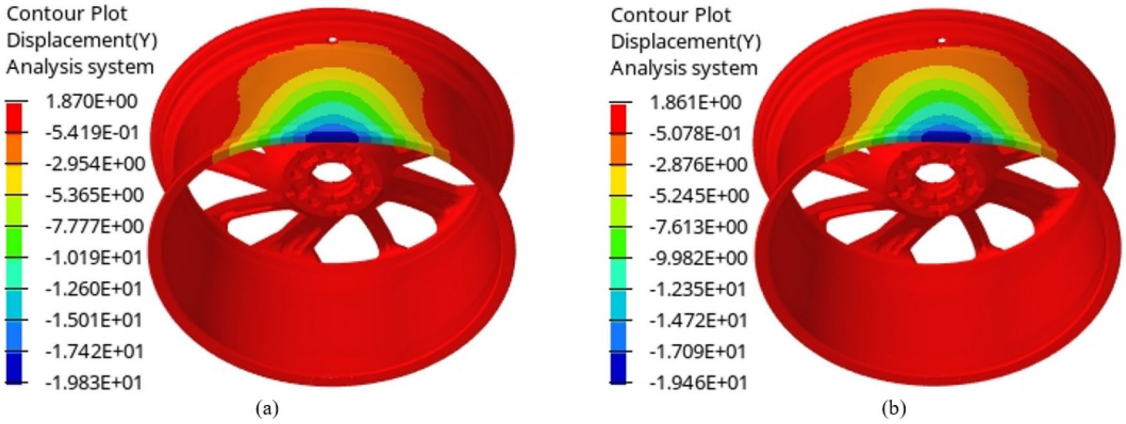

Fig. 24. Optimisation results. (**a**) Before optimisation, (**b**) After optimisation.

Conclusions

The paper presents a novel FE model for simulating the 90° impact test on aluminium alloy wheels based on the QC/T 991–2015 standard. The tyre issue in the 90° impact test was discussed, and the influences of supporting structure, spring and wheel material inhomogeneity were not considered. The hammer was constrained as a rigid body.

The test justified the material parameters so that the FE model could be achieved with better accuracy. The tyre's rubber compound was modelled using a hyper-elastic Yeoh material model. The bead was modelled using an isotropic material. The carcass and belt were modelled as layers of fibre reinforcements embedded in the rubber compound. The improvements in the FE model demonstrated good accuracy and efficiency in the simulation.

The study was conducted in two phases: gaining the best parameters for the simulation and a comparative study. The comparison between the simulations and the tests showed a good agreement with a maximum difference of 7.04% when air leakage was not considered. It is concluded that the FE model developed can effectively replicate the final plastic deformation of the wheel in the 90° impact test.

Also, the study demonstrated the effect of tyres on wheel deformation in the test from an energy perspective. The energy absorbed by the tyre was calculated using the Law of Energy Conservation, which revealed that the higher falling height of the hammer resulted in a lower tyre energy absorption efficiency in the 90° impact test, which is different from the 13° impact test. The rim deformations under two conditions with and without a tyre were analysed, and the results showed that the tyre should be included in the 90° impact test.

Data availability

The datasets analyzed during the current study are available from the corresponding author on reasonable request.

Received: 6 June 2024; Accepted: 30 October 2024
Published online: 08 November 2024

References

1. ISO 3006:2015(E), Road vehicles-Passenger car wheels for road use-Test methods, 2015.
2. ISO 7141:2022, Road vehicles-Light alloy wheels-Lateral impact test, 2022.
3. Automobile Industry Standards of the People's Republic of China. QC/T 991–2015, 90-degree impact test method for light alloy wheels of passenger cars. Standards Press of China, Beijing (2015).
4. Jiménez-Armendáriz, J. et al. Energy dissipation enhancement of thin-walled 6063 T5 aluminium tubes by combining a triggering mechanism and heat treatment. *Metals* **13**(5), 922 (2023).
5. Tang, J. H. et al. An ANSYS/LS-DYNA simulation and experimental study of sectional hob type laver harvesting device. *Agriculture* **13**(2), 361 (2023).
6. Ishikawa S, Sakai Y, Nosaka N. Application of impact analysis for aluminum wheel with inflated tire. SIMULIA Community Conference 2014.
7. Wang, D. F., Zhang, S. & Xu, W. C. Multi-objective optimisation design of wheel based on the performance of 13-degree and 90-degree impact tests. *Int. J. Crashworthiness*. **24**(3), 336–361 (2019).
8. Xu W C, Wang D F. Influence of connecting methods on the 90-degree impact performance of magnesium/aluminum assembled wheel. Int. J. Adhesion and Adhesives.2023;124:103391 (2023).
9. Gao, Q., Shan, Y. C. & Wan, X. F. 90-degree impact bench test and simulation analysis of automotive steel wheel. *Eng. Fail. Anal.* **105**, 143–155 (2019).
10. Previati, G., Ballo, F., Gobbi, M. & Mastinu, G. Radial impact test of aluminum wheels-Numerical and experimental validation. *Int. J. Impact Eng.* **126**, 117–134 (2019).
11. Xiong, W., Tang, J. Q. & Yu, J. H. Research on aluminum alloy wheels's 90-degree impact bench test simulation. *Automotive Parts.* **10**, 41–44 (2019).
12. Shang R, Altenhof, Li N et al. Wheel impact performance with consideration of material inhomogeneity and a simplified approach for modeling. *Int. J Crashworthiness.* **10**(2):137–150 (2005).

13. Tonuk, E. & Unlusoy, Y. S. Prediction of automobile tire cornering force characteristics by finite element modeling and analysis. *Computers and Structures.* **79**(13), 1219–1232 (2001).
14. Neves, R. R. V., Micheli, G. B. & Avlves, M. An experimental and numerical investigation on tire impact. *Int. J. of Impact Eng.* **37**(6), 685–693 (2010).
15. Rafei, M., Ghoreishy, M. H. R. & Naderi, G. Computer simulation of tire rolling resistance using finite element method: effect of linear and nonlinear viscoelastic models. *Proceedings of the Institution of Mechanical Engineers, Part D: J Automobile Eng.* **233**(11), 2746–2760 (2019).
16. Ballo, F., Previati, G. & Mastinu, G. Impact tests of wheels of road vehicles: A comprehensive method for numerical simulation. *Int. J. Impact Eng.* **146**, 103719 (2020).
17. Wan, X. F. et al. Numerical and experimental investigation on the effect of tire on the 13° impact test of automotive wheel. *Adv. in Eng. Software.* **133**, 20–27 (2019).
18. Wang L C. FE-simulation analysis and evaluation of radial tire's transient dynamic characters, South China University of Technology, 2018.
19. Neves, R. R. V., Micheli, G. B. & Alves, M. An experimental and numerical investigation on tire impact. *Int J Impact Eng* **37**(6), 685–693 (2010).
20. Cerit, M. Numerical simulation of dynamic side impact test for an aluminum alloy wheel. *Sci Res Essays* **5**(18), 2694–2701 (2010).
21. Yu Y Y. Research on simulation of impact characteristics of motorcycle wheel. Dissertation, Chongqing University 2019.
22. Orengo F, Ray M H, Plaxico C A. Modeling tire blow-out in roadside hardware simulations using LS-DYNA, ASME International Mechanical Engineering Congress, p. 71–80 (2003).
23. Li, J. et al. Research on the squeeze casting process of large wheel hub based on FEM and RSM. *Int J Adv Manuf Technol* **128**, 197–208 (2023).

Author contributions

S.T. , G.Z. and T.D. wrote the main manuscript text and S.T. prepared figures. L.Z., Y.Z. , J.L., R.L. and S.L., performed Material preparation, data collection and analysis. All authors read and approved the final manuscript. All authors contributed to the study conception and design. All authors reviewed the manuscript.

Funding

This work is supported by the Baoding Science and Technology Plan Project (2394G003), Six Talent Peaks Project in Jiangsu Province,RJFW-051.

Competing interests

The authors declare no competing interests.

Additional information

Correspondence and requests for materials should be addressed to G.Z.